
LOOKING AT MODEL DEBIASING THROUGH THE LENS OF ANOMALY DETECTION

Vito Paolo Pastore*
 MaLGa, DIBRIS
 University of Genoa
 Via Dodecaneso 35, 16129, Genoa, Italy
 vito.paolo.pastore@unige.it

Massimiliano Ciranni*
 MaLGa, DIBRIS
 University of Genoa
 Via Dodecaneso 35, 16129, Genoa, Italy
 massimiliano.ciranni@edu.unige.it

Davide Marinelli
 MaLGa, DIMA
 University of Genoa
 Via Dodecaneso 35, 16129, Genoa, Italy
 davide mari98@gmail.com

Francesca Odone
 MaLGa, DIBRIS
 University of Genoa
 Via Dodecaneso 35, 16129, Genoa, Italy
 francesca.odone@unige.it

Vittorio Murino
 University of Verona, University of Genoa
 Via Dodecaneso 35, 16129, Genoa, Italy
 vittorio.murino@univr.it

July 26, 2024

ABSTRACT

It is widely recognized that deep neural networks are sensitive to bias in the data. This means that during training these models are likely to learn spurious correlations between data and labels, resulting in limited generalization abilities and low performance. In this context, model debiasing approaches can be devised aiming at reducing the model’s dependency on such unwanted correlations, either leveraging the knowledge of bias information or not. In this work, we focus on the latter and more realistic scenario, showing the importance of accurately predicting the bias-conflicting and bias-aligned samples to obtain compelling performance in bias mitigation. On this ground, we propose to conceive the problem of model bias from an out-of-distribution perspective, introducing a new bias identification method based on *anomaly detection*. We claim that when data is mostly biased, bias-conflicting samples can be regarded as outliers with respect to the bias-aligned distribution in the feature space of a biased model, thus allowing for precisely detecting them with an anomaly detection method. Coupling the proposed bias identification approach with bias-conflicting data upsampling and augmentation in a two-step strategy, we reach state-of-the-art performance on synthetic and real benchmark datasets. Ultimately, our proposed approach shows that the data bias issue does not necessarily require complex debiasing methods, given that an accurate bias identification procedure is defined.

1 Introduction

It is commonly acknowledged that deep neural networks can reach outstanding performance when used to tackle several computer vision tasks, including image classification, segmentation, and object detection, to name a few. Nonetheless, their performance is severely affected by the presence of bias in the data. In this case, deep neural networks often rely

*Equally contributing first authors

on spurious correlations between data and labels rather than capturing the semantic features of the objects of interest, leading to poor generalization performance. In this context, *model debiasing* methods have been adopted to reduce the model dependency on the spurious correlations in a biased dataset, enhancing the model capacity to capture semantic target features, while mitigating the bias effect. As an example, let us consider the Waterbirds dataset associated with the binary classification task of predicting images of water and land birds [1]. In this collection, most images of water birds show water in the background, which is generally absent in images of land birds. Consequently, a deep neural network trained on such data learns an undesired shortcut, likely focusing on the background to make predictions, rather than the actual appearance of the birds.

In the last few years, several methods have been proposed to deal with biased datasets. The existing works for bias mitigation either exploit ground-truth bias annotations (regarded as supervised debiasing methods) or do not assume any prior knowledge of the bias (denoted as unsupervised debiasing methods). While supervised approaches operate a finer control over the learning process allowing to selectively mitigate the bias effects, and typically leading to higher performances, unsupervised methods operate blindly, both bias attributes and biased samples are unknown, which is typically the case in a realistic scenario. Among the unsupervised debiasing methods, common approaches leverage 2-stage procedures aiming at, first, detecting the samples affected by the bias (denoted as *bias-aligned*) and those that are not (*bias-conflicting*); and second, applying an actual debiasing process exploiting the estimated (and approximate) split of the data [2, 3, 4, 5, 6]. Empirical evidence shows that the more accurate the prediction of bias-conflicting samples, the higher the generalization performances of the debiased model. This is key to the entire process, yet quite challenging since prior (bias) information is missing, but pervades the large majority of the data, making extremely problematic the detection of the few bias-conflicting samples.

On this ground, we propose that bias-conflicting samples can be considered as outliers in a biased distribution of the feature space inferred by a (biased) model trained on this data. To support our intuition, we train a ResNet-18 model for classification on the training set of Corrupted CIFAR-10, a synthetic biased dataset typically used as a benchmark for model debiasing. We then extract the embeddings of the training set, on which we apply Principal Component Analysis (PCA) for visualization. Then, we input the trained model with bias-conflicting and bias-aligned test samples to extract their embeddings and project them using the same Principal Component (PC) transformation applied to the training set. In Fig. 1, we show the first two PCs of the feature space obtained in this way (green dots for bias-aligned and red dots for bias-conflicting in the figure). For the sake of simplicity, we visualize the feature space for the *Cat* class only. From this figure, one can notice that bias-conflicting samples experience a shift in the feature space distribution of the ResNet-18 model, as compared to the distribution of the bias-aligned ones. This simple example evidences the existence of a distribution shift between bias-conflicting and bias-aligned samples and, given the strong imbalance of such subsets, suggests the usage of an anomaly detection method. Specifically, the shift is limited to the marginal distribution of the embeddings, it is present in each class (in different forms depending on the type of bias), and it can be attributed to a covariate shift in the data [7]. This can be cast as an outlier detection problem, for which anomaly detection methods can be successfully adopted to estimate test samples with covariate shifts [8]. Hence, we propose that an accurate bias-conflicting sample detection can be obtained regarding such samples as anomalies in the embedded feature space of an intentionally biased model. This is in fact a model specifically trained to learn bias-aligned samples, discouraged from learning bias-conflicting samples, and thus amplifying the shift in distribution from the bias-aligned ones.

To sum up, the main contribution of this work is as follows. (i) We claim that bias-conflicting samples generate anomalous feature embeddings in the feature space of a biased model. Thus, we propose the usage of an anomaly detection method for identifying bias-conflicting (and aligned) samples, leveraging an intentionally biased model. To the best of our knowledge, this is the first work that proposes to look at bias-conflicting samples as anomalies, paving the way to the usage of anomaly detection methods for model debiasing tasks, and potentially opening new scenarios to bridge the gap between these two research areas. (ii) We validate our proposed bias-identification approach coupling it with a debiasing method based on predicted bias-conflicting upsampling and data augmentation to fine-tune a model pre-trained on bias data with vanilla ERM. We refer to the resulting two-step method as MoDAD, Model Debiasing with Anomaly Detection. Our results show that our approach based on anomaly detection bias identification reaches competitive performances on a synthetic dataset and state-of-the-art accuracy for three real-world benchmark datasets, obtaining an average improvement of $\sim 3\%$.

The remainder of the paper is organized as follows. In Section 2, we describe relevant literature for model debiasing in image classification. In Section 3, we provide a theoretical background on anomaly detection and details of the proposed approach. Section 4 illustrates the datasets, the evaluation protocol, and implementation details, while also providing the results and ablation analyses. Finally, Section 5 summarizes the proposed method and draws future work.

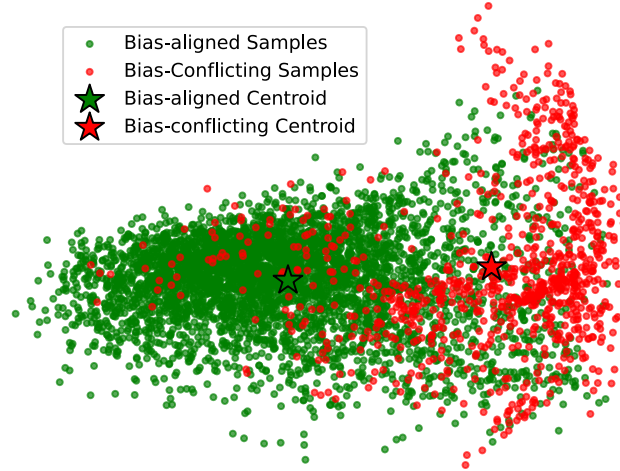


Figure 1: First two PC visualization of bias-aligned (green dots) and bias-conflicting (red dots) ResNet-18 test features from the *Cat* class in Corrupted CIFAR-10.

2 Related Works

The literature addressing data bias and model debiasing is rich, presenting diverse approaches and methodologies that aim at reducing the impact of bias on the generalization capabilities of neural networks. Among them, supervised debiasing methods utilize explicit bias annotations, while unsupervised approaches do not rely on any prior information about the bias. Existing supervised debiasing methods include distributionally robust optimization [1], and bias feature disentanglement [9]. In ReBias, Bahng *et al.* [10] propose an approach relying on prior knowledge on the bias rather than bias labels. Wang *et al.* [11] introduce HEX, a method based on a differentiable neural building block, to reduce dependence on image textural information.

We focus on state-of-the-art analysis on unsupervised debiasing approaches, which share the same high-level structure of our proposed method. Nam *et al.* [12] propose an architecture based on two models. The first model is intentionally biased using a generalized cross-entropy loss function, while a second model is jointly trained with the first one with a weighted cross-entropy loss function, under the assumption that bias-conflicting samples would contribute more to the loss than the bias-aligned ones. Lee *et al.* [13] demonstrate the importance of training a model with diverse bias-conflicting samples, proving that “diversity” outperforms oversampling. They synthesize diverse bias-conflicting samples from the bias-aligned ones.

Among the unsupervised methods, a common approach involves the usage of two-step algorithms, where the first step consists in estimating the correct split between bias-conflicting and bias-aligned samples, which is further exploited for debiasing the model, typically devoting more importance to bias-conflicting samples during training. In [2], a model with an early stopping criterion based on explicit bias information in a validation set is first trained. The model’s misclassified samples are then selected as bias-conflicting, and a second model is trained with a weighted cross-entropy loss function, whose weights are set proportionally to the number of identified bias-aligned and conflicting samples. Kim *et al.* [4] provide a data augmentation framework to generate “bias-swapped” images, accounting for the bias attributes from the bias-conflicting images, and the bias-irrelevant attributes from the bias-aligned samples. Their proposed bias identification strategy consists in assigning a bias score to each sample based on both the classification correctness and model confidence, using a model trained with Generalized Cross-Entropy (GCE) loss. Seo *et al.* [14] propose a method based on feature clustering and cluster re-weighting, starting from the observation that examples with the same bias attributes tend to have similar representations in the feature space. In [5], assuming that the training samples are partitioned into domains or environments, the authors aim to find environments that maximally violate the invariant learning principle. In these environments, the reference classifier associates the same feature vector with examples of different classes. Features that are domain-invariant predict the true class regardless of the domain. A similar bias identification approach is used in [6]. In [3], the hidden stratification phenomenon is tackled, which happens when classes comprise multiple finer-grained sub-classes. The identification of the sub-classes is achieved through feature clustering applied on a model trained on the super-class classification task.

Differently from the above works, MoDAD is a two-step debiasing method that, first, leverages the accurate identification of bias-conflicting samples regarded as anomalies in the feature space of an intentionally biased model, due to a distribution shift with respect to the more numerous bias-aligned ones. Consequently, MoDAD exploits an anomaly

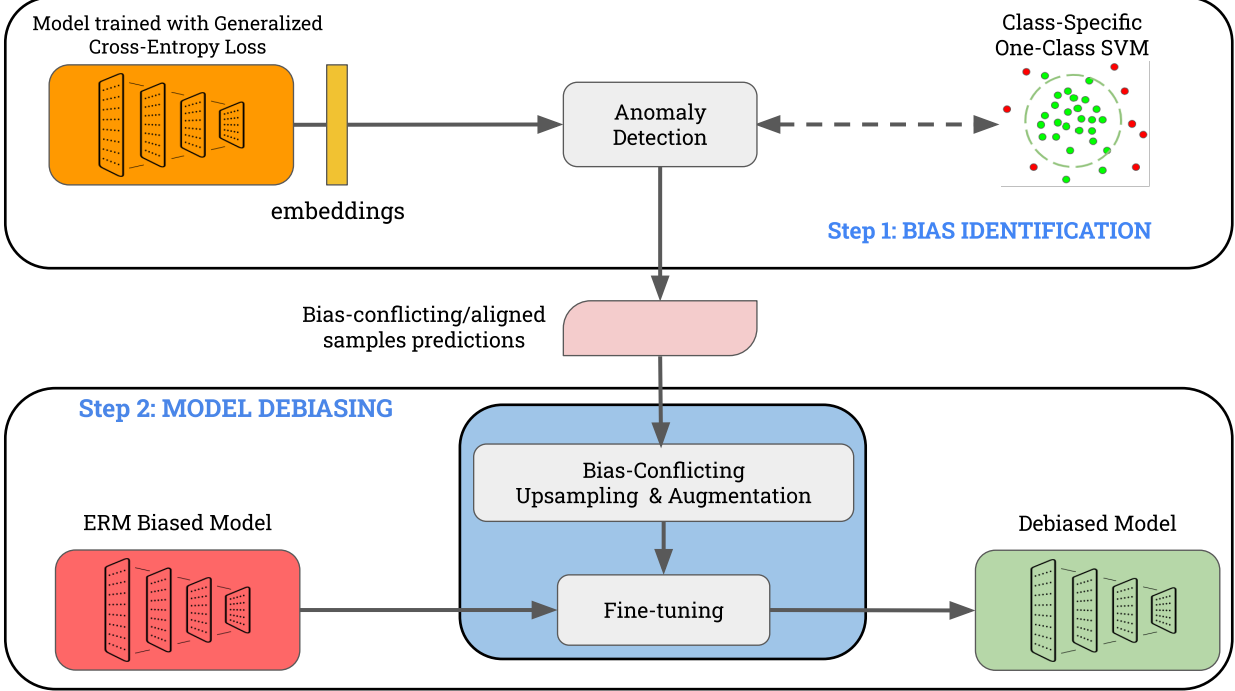


Figure 2: Schematic representation of our two-step method (MoDAD).

detection algorithm for identifying the correct split of bias-conflicting and bias-aligned samples. Second, in the actual MoDAD’s debiasing step, a biased model is fine-tuned using the bias-conflicting and bias-aligned sample estimates to mitigate the bias dependence.

3 Approach

In this section, we describe the core part of this study. First, we detail the problem setting and outline the intuition supporting our bias-identification approach. Then, we describe the customized anomaly detection method employed in our experiments and the debiasing approach implemented for supporting the anomaly detection-based bias identification procedure.

3.1 Problem Formulation

Let us consider an image classification problem, where a dataset $\mathcal{D} = \{(x_0, y_0), (x_1, y_1), \dots, (x_n, y_n)\}$, for which every pair (x_i, y_i) represents an input image and its associated semantic target label, is used to train a model f_θ to output \hat{y} as the correct class of an unseen sample x_{new} by minimizing an ERM objective. If the training set \mathcal{D} presents a bias and the model is naively trained, f_θ likely learns shortcuts based on spurious correlations between samples and target classes instead of the actual semantic attributes [12]. In a biased dataset, most samples present these spurious correlations (i.e., are biased-aligned), while only a small portion does not (i.e., bias conflicting), by definition. Consequently, the model naively trained on a biased dataset shows poor generalization performance when tested on new data drawn from an *unbiased* distribution, as it memorizes the few bias-conflicting samples present in the training set instead of properly learning their semantics.

In this scenario, we can expect that the bias-aligned samples of a certain training class are compact, showing high density in the model’s feature space, as they share bias attributes. Intuitively, the distribution $p(X|Y)$ of a biased training class will be skewed, with the bias-aligned samples being concentrated in the main mode (a wide peak) and the bias-conflicting belonging to the (potentially long) tails of such distribution. This is the typical setting for Anomaly Detection, defined as the task of revealing uncharacteristic samples in a data set, defined as anomalies or outliers. Anomaly Detection methods can effectively learn a margin separating the samples in the high-density

Algorithm 1 Pseudocode of the proposed bias identification step

1: **Input:**
 An image training set $\mathcal{D} \subseteq \mathcal{X} \times \mathcal{Y} = \{(x_1, y_1), \dots, (x_N, y_N)\}$,
 A Neural Network f_θ with randomly initialized weights θ , with $f_\theta := \Phi \circ h$,
 where Φ is a DNN backbone and h a NN classifier,
 2: **Output:** $\hat{\mathcal{B}} :=$ bias-aligned and bias-conflicting samples estimation.

3: Define a Weighted Random Sampler \mathcal{S} , weighting each sample (x_i, y_i) with the inverse of its class population ψ_{y_i} , and set *replacement*=True if class populations are uneven, False otherwise.
 4: Train f_θ with GCE Loss.
 5: Extract training samples embeddings $\mathcal{Z} = \{(\Phi(x), y), \forall (x, y) \in \mathcal{D}\}$.
 6: For each class, fit a separate OCSVM $_y$ on the $\Phi(x)$ of samples from that class correctly classified by f_θ , denoted as \mathcal{C}_y .
 7: Compute the anomaly scores of each class samples \mathcal{A}_y with OCSVM $_y$
 8: Compute a decision threshold τ_y as the anomaly score corresponding to Percentile(\mathcal{A}_y, α_y), $\alpha_y = 100 \cdot \frac{1}{2} \left(\frac{\psi_y - |\mathcal{C}_y|}{\psi_y} \right)$
 9: $\hat{\mathcal{B}}_i = \text{bool}(\mathcal{A}_y[\Phi(x)]) > \tau_y$

region (bias-aligned) from the samples belonging to the distribution’s tails, which will fall outside of it, as they are in lower-density regions (bias-conflicting).

Hence, we claim it is possible to identify bias-conflicting samples in a biased dataset as the samples inducing *anomalous* features in a biased model. To this end, we exploit and customize a well-established anomaly detection algorithm, One-Class Support Vector Machine (OCSVM) [15], to design a *bias identification* procedure capable of identifying conflicting samples with high accuracy. The use of OCSVM stems from its effectiveness, efficiency, and controllability, while we leave to future work investigating Deep Anomaly Detection approaches for this task.

3.2 OCSVM Customization and Bias Identificaton

3.2.1 OCSVM customization

Several Anomaly Detection (AD) methods have been proposed, either relying on deep learning [16] or traditional machine learning approaches [17, 18, 15]. In this work, we aim to frame the problem of unknown bias identification in the context of anomaly detection, and we opt to exploit the One-Class Support Vector Machine (OCSVM). It can be regarded as an unsupervised technique that learns a hyperplane separating the training samples from the origin while maximizing the hyperplane distance from it, and which can learn meaningful margins without the need for manual annotations [15, 19]. In the context of dataset bias, its associated decision function would ideally return $+1$ for in-class (bias-aligned) samples and -1 for samples detected as anomalous (bias-conflicting).

$$f(x) = \text{sign} \left(\sum_{i=1}^m \alpha_i K(x, x_i) - \lambda \right) \quad (1)$$

Such decision function is outlined in Eq. (1), where α_i and λ are the learned Lagrange multipliers and hyperplane’s offset respectively, while K is the Gram matrix of distances between sample points in kernel space. The higher the argument of the *sign*, the higher the (signed) distance of a sample from the learned margin, with a positive distance indicating that a sample should be regarded as in-class (positive sign), or out-of-class (negative sign). As such, the argument of the *sign*, can be regarded as an *anomaly score*.

In our bias identification approach, we modify Eq. (1) to shift the argument of the *sign* by a threshold τ (which we automatically compute, see Algorithm 1), so that when the anomaly score is higher than τ the corresponding sample is classified as in-class, and anomalous otherwise. Such a decision threshold can be used to restrict anomaly predictions with respect to the original formulation. In our approach, we train one OCSVM per target class, allowing us to tailor bias detection specifically to individual categories.

3.2.2 Amplifying the distribution shift with GCE

Naively training a model on a biased dataset produces a biased classifier, learning the spurious correlations between samples and target classes, representative of bias. However, after just a few epochs ([2]) the model typically overfits the training samples, memorizing bias-conflicting samples as well. Consequently, the actual distribution shift between

bias-conflicting and bias-aligned samples in the biased model’s feature space disappears. To overcome this issue while being robust with respect to the number of training iterations, we employ the Generalized Cross Entropy (GCE) [20] as our loss function for the bias identification step. As shown in [12, 4], GCE loss makes the model to *attach* onto bias, weighting the samples that the model classifies with high confidence (i.e., bias-aligned) more than the uncertain ones (i.e., bias-conflicting). However, differently from [12, 4], we use GCE to further amplify the distribution shift between bias-aligned and bias-conflicting samples, avoiding bias-conflicting sample memorization and favoring their identification with anomaly detection algorithms.

3.3 Bias Mitigation: Fine-Tuning the Biased Model

In this work, we design a debiasing scheme based on *bias-conflicting upsampling and augmentation* (see Fig. 2). Starting from a model trained using the biased dataset with vanilla ERM and hence likely biased, we employ a *weighted random sampler* with replacement, whose weights are set depending on the prediction \hat{B} of the bias identification step, as the inverse of the two estimated populations.

With this sampler, during the debiasing training process, we build each mini-batch such that the ratio of bias-aligned and bias-conflicting samples is roughly balanced. We further perform upsampling adding three augmented images for each bias-conflicting sample in each mini-batch, so that the number of bias-conflicting samples in the batch results 4 times higher than the number of bias-aligned ones. Exploiting this batch construction scheme, a classic CE loss function is then used for debiasing a model. Differently from other two-step methods (e.g., JTT [2]), MoDAD performs the debiasing process on an already biased model, facing a realistic scenario when bias is unknown.

4 Experiments

In this section, we report an extensive experimental analysis, encompassing the description of the employed synthetic and realistic datasets, the evaluation protocol adopted, the obtained performance and comparisons, and ablation studies. Readers may refer to the Supplementary Materials for further information on implementation details, and data pre-processing.

4.1 Datasets

To validate our approach, we consider a *synthetic* (CIFAR-10) and three *realistic* (BAR, BFFHQ, Waterbirds) datasets. The synthetic dataset allows the test of the algorithm under controlled varying conditions, specifically the knowledge of the bias and in which percentage it affects the data. In realistic datasets, instead, prior information regarding bias could not be available, while potentially presenting additional challenges including unbalanced per-class populations, and erroneous annotations, to name a few.

Corrupted CIFAR-10 is the first investigated dataset in the version made available from [13]. This dataset is derived from the original 10-class CIFAR-10 [21], composed of 60,000 images altered by 10 different types of corruptions following the protocol introduced by [22]. Such image corruptions are $\{ \text{Snow, Frost, Fog, Brightness, Contrast, Spatter, Elastic, JPEG, Pixelate, Saturate} \}$, each one being highly correlated with the ten semantic labels. We consider three degrees of correlation ρ corresponding to $\{0.950, 0.980, 0.995\}$. The train and validation sets have the same correlation ρ between bias-attribute and semantic label, while in the test set 90% are bias-conflicting and only 10% have spurious correlations with the label. Figure 3 shows some examples from this dataset.

BAR (Biased Action Recognition) is an action recognition image dataset with a strong correlation between the performed action and the setting in which it is carried out. It was introduced in [12] and consists of six different semantic classes



Figure 3: Example of bias-aligned (left) and bias-conflicting samples (right) from Corrupted CIFAR-10 Dataset.



Figure 4: Example of bias-aligned (top) and bias-conflicting samples (bottom) from BAR dataset.

(*Climbing, Diving, Fishing, Racing, Throwing, Vaulting*), for a total of 2,595 images. The samples are further divided into a training set of 1,941 images and a test set of 654 images with no pre-defined validation set. For example, the *Climbing* class contains a great majority of images in the training set where the subject is performing rock climbing. In contrast, in the test set, we can find many images of people climbing on snow or ice (see Figure 4). Additionally, this dataset does not provide ground-truth annotation regarding whether a sample is bias-aligned or bias-conflicting.

BFFHQ is a visually perceived gender-biased image dataset of human faces, obtained from the Flickr-Faces-HQ dataset [23]. Introduced in [4], we refer to the version made publicly available from [13]. It is characterized by two target attributes related to age (*Young* and *Old*), where the great majority of training samples are either young female faces or old male faces (bias-aligned), while a small minority are old females or young males (bias-conflicting). This correlation is broken in the validation and test sets, where the two attributes are uniformly distributed. It totals 21,200 images where 19,200 images are used as training samples, 1,000 samples for validation and 1000 samples for testing. Samples of this dataset are shown in Figure 5.

Waterbirds is an image dataset introduced in [1] that combines *bird* subjects from the Caltech-UCSD Birds-200-2011 (CUB) dataset [24] and image backgrounds from the Places dataset [25]. Images are divided according to a target attribute regarding birds being Waterbirds or Landbirds, while the background being land or water represents the bias attribute. In this setting, images depicting Landbirds on land and Waterbirds on water are bias-aligned samples, whereas pairing a Landbird with a water background constitutes a bias-conflicting sample (and vice-versa for Waterbirds on land background).

4.2 Evaluation Protocol

We employ two quantitative metrics in our results: *Average Accuracy* and *Conflicting Accuracy*. Average Accuracy is the accuracy over the whole test set, which typically contains a balanced number of bias-aligned and conflicting samples, except otherwise stated. Conflicting Accuracy refers to the average accuracy computed only on the bias-conflicting data. We provide the mean and standard deviation of three independent runs for each experiment. For the comparative analysis, we follow the same evaluation protocol of Lee *et al.*[13] for Corrupted CIFAR-10, as we employ the very same version of this dataset, thus reporting the Average Accuracy of the whole test set. The test sets of BFFHQ and Waterbirds are balanced, containing an equal percentage of bias-aligned and bias-conflicting samples. For the BAR dataset, we report just the Average Accuracy due to the absence of bias annotations preventing us from computing



Figure 5: Example of bias-aligned (left) and bias-conflicting samples (right) from BFFHQ dataset.

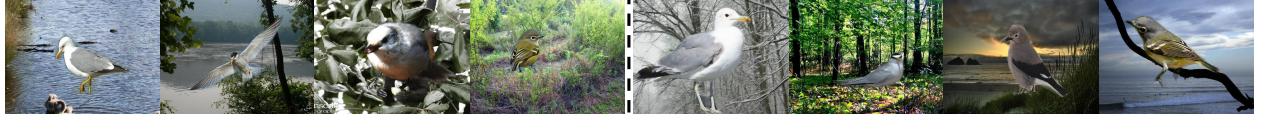


Figure 6: Example of bias-aligned (left) and bias-conflicting samples (right) from Waterbirds dataset.

separate metrics. Finally, as a baseline, we also report the performance of a model trained without any debiasing strategy, i.e. through Empirical Risk Minimization [26] with standard cross-entropy loss.

4.3 Results

Training Details For the sake of comparison, we employ a ResNet-18 [27] for Corrupted CIFAR-10, BAR, and BFFHQ, like in [4, 2, 13]. In the experiments involving Waterbirds, we opt to use a ResNet-50 as in [1]. For the real-world datasets, we start from a model whose weights are pre-trained on ImageNet [28], like in [13, 12, 2]. For each model, we plug on top of the last backbone layer an MLP with one hidden layer followed by a ReLU. About the OCSVM, we set the contamination parameter to 0.5 and adopt a Radial Basis Function (RBF) kernel. For all the other technical details, please refer to the Supplementary Material.

4.3.1 Corrupted CIFAR-10.

Table 1 provides MoDAD’s results on three different ρ values of Corrupted CIFAR-10, benchmarking with relevant existing approaches. Despite the basic debiasing step, our method is competitive with respect to state-of-the-art approaches for the three different bias ratios, reaching similar performances of DFA [13] and LfF [12], while being slightly lower for $\rho = 0.995$. Please, note that our performance result is more stable considering the standard deviation, which is an order of magnitude lower than that of the other methods. Moreover, we significantly outperform JTT [2], whose debiasing approach is similar to the one employed in MoDAD, for all the bias ratios, further suggesting the effectiveness of our bias identification mechanism. Regarding the accuracy of our anomaly detection algorithm in bias identification, the average and standard deviation for the F1-score over the ten corrupted CIFAR-10 classes, correspond to 0.81 ± 0.05 , 0.80 ± 0.07 and 0.68 ± 0.11 , for $\rho = \{0.950, 0.980, 0.995\}$ respectively (see Table 2). Finally, in the last entry of Table 1 we report the oracle represented by using the ground truth bias labels and our proposed debiasing method. The reported oracle accuracy provides the best performances among the referenced methods, confirming our intuition regarding the importance of precise bias identification for model debiasing.

Method	BS	Corrupted CIFAR-10		
		$\rho = 0.995$	$\rho = 0.980$	$\rho = 0.950$
ERM+CE	–	21.43 ± 0.57	30.37 ± 1.37	39.88 ± 0.70
HEX [11]	✓	13.87 ± 0.06	15.20 ± 0.54	16.04 ± 0.63
EnD [9]	✓	22.89 ± 0.27	31.31 ± 0.35	40.26 ± 0.85
ReBias [10]	✓	22.27 ± 0.41	31.66 ± 0.43	43.43 ± 0.41
BiaSwap [4]	✗	$29.11 \pm --$	$35.25 \pm --$	$41.62 \pm --$
LfF [12]	✗	28.81 ± 0.44	40.66 ± 0.70	50.72 ± 1.31
JTT [2]	✗	23.66 ± 0.78	31.44 ± 0.47	41.20 ± 0.19
DFA [13]	✗	29.95 ± 0.71	41.78 ± 2.29	51.13 ± 1.28
Ours	✗	27.26 ± 0.47	41.27 ± 0.26	50.48 ± 0.42
Ours (Oracle)	✓	35.98 ± 0.83	45.47 ± 0.83	53.84 ± 0.62

Table 1: MoDAD’s Average Accuracy on Corrupted CIFAR-10 and related comparisons. BS refers to Bias Supervision. Best results in bold.

Dataset	ρ	F1-Score
Corrupted CIFAR-10	0.950	0.81 ± 0.05
Corrupted CIFAR-10	0.980	0.80 ± 0.07
Corrupted CIFAR-10	0.995	0.68 ± 0.11
Waterbirds	0.950	0.70 ± 0.07
BFFHQ	0.995	0.75 ± 0.05

Table 2: F1-Score of our per-class Bias Identification method (standard deviation refers to the target classes)

Method	BS	BAR		Waterbirds		BFFHQ	
		Average	Conflicting	Average	Conflicting	Average	Conflicting
ERM+CE	–	58.00 ± 1.39	–	91.20 ± 0.76	84.31 ± 1.53	79.77 ± 0.23	60.13 ± 0.46
GroupDRO [1]	✓	–	–	$93.50 \pm \text{--}$	$91.4 \pm \text{--}$	–	–
BiaSwap [4]	✗	$52.44 \pm \text{--}$	–	–	–	–	$58.87 \pm \text{--}$
LfF [12]	✗	62.98 ± 2.76	–	$97.50 \pm \text{--}$	$75.20 \pm \text{--}$	75.23 ± 1.60	62.97 ± 3.22
JTT [2]	✗	68.53 ± 3.29	–	$93.60 \pm \text{--}$	$86.00 \pm \text{--}$	80.93 ± 0.69	62.20 ± 1.34
DFA [13]	✗	–	–	–	–	–	63.87 ± 0.31
EIIL [29]	✗	$65.44 \pm \text{--}$	–	$96.90 \pm \text{--}$	$78.70 \pm \text{--}$	–	59.20 ± 1.90
George [30]	✗	–	–	95.50 ± 2.00	$76.20 \pm \text{--}$	–	–
DebiAN [31]	✗	69.88 ± 2.92	–	–	–	–	62.80 ± 0.60
Ours	✗	69.83 ± 0.72	–	93.52 ± 0.73	89.43 ± 1.69	83.50 ± 1.39	68.33 ± 2.89
Ablation w\ JTT	✗	63.25 ± 0.38	–	93.00 ± 0.09	87.93 ± 0.13	80.20 ± 0.02	61.13 ± 0.12

Table 3: MoDAD’s performance on realistic image datasets. For BAR, only the average accuracy is reported, as its annotations do not contain information regarding which samples are either bias-aligned or bias-conflicting. BS refers to Bias Supervision. The best results are in bold.

4.3.2 Realistic Datasets

Table 3 reports the performance of MoDAD and a comparison with relevant existing works on the three real-world datasets. First, we evaluate the accuracy of our bias-identification approaches on Waterbirds and BFFHQ, obtaining an average f1-score of 0.70 and 0.75, respectively (see Table 2). Regarding the debiasing performance, MoDAD surpasses other unsupervised debiasing works, apart from the Average Accuracy on Waterbirds, where LfF [12] reports the highest among all the works in this category. At the same time, our method reaches higher Conflicting Accuracy, almost matching the supervised state-of-the-art on this dataset (GroupDRO [1]). Regarding BAR, we match the performance of DebiAN [31] (–0.05%) on average, but with a significantly lower standard deviation (2.92 for DebiAN, 0.72 for MoDAD). BFFHQ has a bias-correlation $\rho = 0.995$, thus capturing the contribution of the few bias-conflicting training is much harder. However, in BFFHQ we report the most significant improvement over existing works, with a Conflicting Accuracy of 68.33%, corresponding to an improvement of 4.46% over the second-best approach (DFA [13]).

4.4 Ablation Studies

AD Algorithm	Average Accuracy
COV	44.34 ± 0.29
IFO	44.95 ± 0.61
LOF	49.10 ± 0.13
OCSVM	$50.48 \pm \pm 0.62$

Table 4: MoDAD’s performance on Corrupted CIFAR10 ($\rho = 0.950$) with different anomaly detection algorithms

In this section, we report ablation studies to evaluate the impact of our design choices on the proposed methodology. Additional analyses can be found in the Supplementary.

Bias identification method. To further support the effectiveness of our anomaly detection-based bias identification procedure, we perform an ablation study on our bias identification method. Specifically, we run our debiasing step using bias-aligned and bias-conflicting predictions obtained with the original implementation of JTT [2]. The last entry of Table 3 summarizes the obtained results. On three runs, we obtain an average decrease in the debiased model performance corresponding to 1.63% and 7.20% for the Conflicting accuracy in Waterbirds and BFFHQ, respectively, and 6.58% in Average accuracy for BAR. The obtained results further support the impact of the anomaly detection method for identifying bias in the performance of the final debiased model.

Anomaly detection algorithm. To show the soundness of the proposed approach regardless of the anomaly detection method adopted, we perform several tests by using other readily available anomaly detectors, on the Corrupted CIFAR-10 dataset (with $\rho = 0.950$). Specifically, we consider the *Local Outlier Factor* (LOF) [32], the *Isolation Forest* (IFO) [33], and the *Robust Covariance Estimator* (COV) [34]. Table 4 reports the average accuracy on Corrupted CIFAR-10 with $\rho = 0.950$. OCSVM is indeed the best option among the considered ones. However, the obtained results confirm that changing the detector has only a modest impact on the results, demonstrating that the intuition regarding bias-conflicting samples as anomalies does not indeed depend on our specific design choice of the anomaly detection method.

5 Conclusions

Deep neural networks typically exhibit poor generalization performances when bias is present in the data. In these cases, they likely rely on misleading correlations between bias and labels rather than the desired correlations representing the semantics of a certain class. Model debiasing consists in methods for mitigating the model’s prediction dependency on bias. In this work, we consider an unsupervised debiasing framework, meaning that no knowledge of bias is used, simulating a realistic scenario. We claim that bias-conflicting samples produce features that are anomalous in the feature space of an intentionally biased model. Thus, we propose to use anomaly detection methods for bias identification, filling the gap between model debiasing and anomaly detection, and potentially opening new research directions. To validate the proposed strategy, we embed it into a two-step method named MoDAD, where the bias-aligned and bias-conflicting samples, identified through the anomaly detection scheme, are used for model debiasing. Specifically, our model debiasing consists in fine-tuning a biased model (trained with vanilla ERM) exploiting bias-conflicting upsampling and augmentation. Our results show that MoDAD can reach competitive performance on benchmark datasets, slightly outperforming state-of-the-art methods based on more complicated debiasing approaches, empirically proving the effectiveness of the anomaly detection bias identification strategy.

References

- [1] Shiori Sagawa, Pang Wei Koh, Tatsunori B Hashimoto, and Percy Liang. Distributionally robust neural networks. In *International Conference on Learning Representations*, 2019.
- [2] Evan Z Liu, Behzad Haghgoo, Annie S Chen, Aditi Raghunathan, Pang Wei Koh, Shiori Sagawa, Percy Liang, and Chelsea Finn. Just train twice: Improving group robustness without training group information. In *International Conference on Machine Learning*, pages 6781–6792. PMLR, 2021.
- [3] Nimit Sohoni, Jared Dunnmon, Geoffrey Angus, Albert Gu, and Christopher Ré. No subclass left behind: Fine-grained robustness in coarse-grained classification problems. *Advances in Neural Information Processing Systems*, 33:19339–19352, 2020.
- [4] Eungyeup Kim, Jihyeon Lee, and Jaegul Choo. Biaswap: Removing dataset bias with bias-tailored swapping augmentation. In *Proceedings of the IEEE/CVF International Conference on Computer Vision*, pages 14992–15001, 2021.
- [5] Elliot Creager, Jörn-Henrik Jacobsen, and Richard Zemel. Environment inference for invariant learning. In *International Conference on Machine Learning*, pages 2189–2200. PMLR, 2021.
- [6] Faruk Ahmed, Yoshua Bengio, Harm Van Seijen, and Aaron Courville. Systematic generalisation with group invariant predictions. In *International Conference on Learning Representations*, 2020.
- [7] Nimisha G Nair, Pallavi Satpathy, Jabez Christopher, et al. Covariate shift: A review and analysis on classifiers. In *2019 Global Conference for Advancement in Technology (GCAT)*, pages 1–6. IEEE, 2019.
- [8] Jingkang Yang, Kaiyang Zhou, Yixuan Li, and Ziwei Liu. Generalized out-of-distribution detection: A survey, 2024.

- [9] Enzo Tartaglione, Carlo Alberto Barbano, and Marco Grangetto. End: Entangling and disentangling deep representations for bias correction. In *Proceedings of the IEEE/CVF Conference on Computer Vision and Pattern Recognition (CVPR)*, pages 13508–13517, June 2021.
- [10] Hyojin Bahng, Sanghyuk Chun, Sangdoo Yun, Jaegul Choo, and Seong Joon Oh. Learning de-biased representations with biased representations. In *International Conference on Machine Learning*, pages 528–539. PMLR, 2020.
- [11] Haohan Wang, Zexue He, and Eric P. Xing. Learning robust representations by projecting superficial statistics out. In *International Conference on Learning Representations*, 2019.
- [12] Junhyun Nam, Hyuntak Cha, Sungsoo Ahn, Jaeho Lee, and Jinwoo Shin. Learning from failure: De-biasing classifier from biased classifier. *Advances in Neural Information Processing Systems*, 33:20673–20684, 2020.
- [13] Jungsoo Lee, Eungyeup Kim, Juyoung Lee, Jihyeon Lee, and Jaegul Choo. Learning debiased representation via disentangled feature augmentation. In M. Ranzato, A. Beygelzimer, Y. Dauphin, P.S. Liang, and J. Wortman Vaughan, editors, *Advances in Neural Information Processing Systems*, volume 34, pages 25123–25133. Curran Associates, Inc., 2021.
- [14] Seonguk Seo, Joon-Young Lee, and Bohyung Han. Unsupervised learning of debiased representations with pseudo-attributes. In *Proceedings of the IEEE/CVF Conference on Computer Vision and Pattern Recognition*, pages 16742–16751, 2022.
- [15] Bernhard Schölkopf, John C Platt, John Shawe-Taylor, Alex J Smola, and Robert C Williamson. Estimating the support of a high-dimensional distribution. *Neural computation*, 13(7):1443–1471, 2001.
- [16] Guansong Pang, Chunhua Shen, Longbing Cao, and Anton Van Den Hengel. Deep learning for anomaly detection: A review. *ACM computing surveys (CSUR)*, 54(2):1–38, 2021.
- [17] Fei Tony Liu, Kai Ming Ting, and Zhi-Hua Zhou. Isolation forest. In *2008 eighth ieee international conference on data mining*, pages 413–422. IEEE, 2008.
- [18] Determinant EStimator. A fast algorithm for the minimum covariance. *Technometrics*, 41(3):212, 1999.
- [19] Bouchra Lamrini, Augustin Gjini, Simon Daudin, Pascal Pratmarty, François Armando, and Louise Travé-Massuyès. Anomaly detection using similarity-based one-class svm for network traffic characterization. In *DX*, 2018.
- [20] Zhilu Zhang and Mert Sabuncu. Generalized cross entropy loss for training deep neural networks with noisy labels. In S. Bengio, H. Wallach, H. Larochelle, K. Grauman, N. Cesa-Bianchi, and R. Garnett, editors, *Advances in Neural Information Processing Systems*, volume 31. Curran Associates, Inc., 2018.
- [21] Alex Krizhevsky, Geoffrey Hinton, et al. Learning multiple layers of features from tiny images. 2009.
- [22] Dan Hendrycks and Thomas Dietterich. Benchmarking neural network robustness to common corruptions and perturbations. In *International Conference on Learning Representations*, 2019.
- [23] Tero Karras, Samuli Laine, and Timo Aila. A style-based generator architecture for generative adversarial networks. In *Proceedings of the IEEE/CVF conference on computer vision and pattern recognition*, pages 4401–4410, 2019.
- [24] C. Wah, S. Branson, P. Welinder, P. Perona, and S. Belongie. Cub-200-2011 tech report. Technical Report CNS-TR-2011-001, California Institute of Technology, 2011.
- [25] Bolei Zhou, Agata Lapedriza, Jianxiong Xiao, Antonio Torralba, and Aude Oliva. Learning deep features for scene recognition using places database. In Z. Ghahramani, M. Welling, C. Cortes, N. Lawrence, and K.Q. Weinberger, editors, *Advances in Neural Information Processing Systems*, volume 27. Curran Associates, Inc., 2014.
- [26] V. Vapnik. Principles of risk minimization for learning theory. In J. Moody, S. Hanson, and R.P. Lippmann, editors, *Advances in Neural Information Processing Systems*, volume 4. Morgan-Kaufmann, 1991.
- [27] Kaiming He, Xiangyu Zhang, Shaoqing Ren, and Jian Sun. Deep residual learning for image recognition. In *Proceedings of the IEEE Conference on Computer Vision and Pattern Recognition (CVPR)*, June 2016.
- [28] Jia Deng, Wei Dong, Richard Socher, Li-Jia Li, Kai Li, and Li Fei-Fei. Imagenet: A large-scale hierarchical image database. In *2009 IEEE Conference on Computer Vision and Pattern Recognition*, pages 248–255, 2009.
- [29] Elliot Creager, Jörn-Henrik Jacobsen, and Richard Zemel. Environment inference for invariant learning. In *International Conference on Machine Learning*, pages 2189–2200. PMLR, 2021.
- [30] Nimit Sohoni, Jared Dunnmon, Geoffrey Angus, Albert Gu, and Christopher Ré. No subclass left behind: Fine-grained robustness in coarse-grained classification problems. *Advances in Neural Information Processing Systems*, 33:19339–19352, 2020.

- [31] Zhiheng Li, Anthony Hoogs, and Chenliang Xu. Discover and mitigate unknown biases with debiasing alternate networks. In *European Conference on Computer Vision*, pages 270–288. Springer, 2022.
- [32] Markus M. Breunig, Hans-Peter Kriegel, Raymond T. Ng, and Jörg Sander. Lof: Identifying density-based local outliers. *SIGMOD Rec.*, 29(2):93–104, may 2000.
- [33] Fei Tony Liu, Kai Ming Ting, and Zhi-Hua Zhou. Isolation forest. In *Proceedings of the 2008 Eighth IEEE International Conference on Data Mining, ICDM '08*, page 413–422, USA, 2008. IEEE Computer Society.
- [34] Peter Rousseeuw and Katrien Driessen. A fast algorithm for the minimum covariance determinant estimator. *Technometrics*, 41:212–223, 08 1999.
- [35] Guido Van Rossum and Fred L. Drake. *Python 3 Reference Manual*. CreateSpace, Scotts Valley, CA, 2009.
- [36] Adam Paszke, Sam Gross, Francisco Massa, Adam Lerer, James Bradbury, Gregory Chanan, Trevor Killeen, Zeming Lin, Natalia Gimelshein, Luca Antiga, Alban Desmaison, Andreas Kopf, Edward Yang, Zachary DeVito, Martin Raison, Alykhan Tejani, Sasank Chilamkurthy, Benoit Steiner, Lu Fang, Junjie Bai, and Soumith Chintala. Pytorch: An imperative style, high-performance deep learning library. In H. Wallach, H. Larochelle, A. Beygelzimer, F. d’Alché-Buc, E. Fox, and R. Garnett, editors, *Advances in Neural Information Processing Systems*, volume 32. Curran Associates, Inc., 2019.
- [37] TorchVision maintainers and contributors. Torchvision: Pytorch’s computer vision library. <https://github.com/pytorch/vision>, 2016.
- [38] F. Pedregosa, G. Varoquaux, A. Gramfort, V. Michel, B. Thirion, O. Grisel, M. Blondel, P. Prettenhofer, R. Weiss, V. Dubourg, J. Vanderplas, A. Passos, D. Cournapeau, M. Brucher, M. Perrot, and E. Duchesnay. Scikit-learn: Machine learning in Python. *Journal of Machine Learning Research*, 12:2825–2830, 2011.
- [39] Charles R. Harris, K. Jarrod Millman, Stéfan J. van der Walt, Ralf Gommers, Pauli Virtanen, David Cournapeau, Eric Wieser, Julian Taylor, Sebastian Berg, Nathaniel J. Smith, Robert Kern, Matti Picus, Stephan Hoyer, Marten H. van Kerkwijk, Matthew Brett, Allan Haldane, Jaime Fernández del Río, Mark Wiebe, Pearu Peterson, Pierre Gérard-Marchant, Kevin Sheppard, Tyler Reddy, Warren Weckesser, Hameer Abbasi, Christoph Gohlke, and Travis E. Oliphant. Array programming with NumPy. *Nature*, 585(7825):357–362, September 2020.
- [40] J. D. Hunter. Matplotlib: A 2d graphics environment. *Computing in Science & Engineering*, 9(3):90–95, 2007.
- [41] Ilya Loshchilov and Frank Hutter. Decoupled weight decay regularization. In *International Conference on Learning Representations*, 2019.

Appendix

S1. Additional Ablation Studies

S1.1 Contribution of the per-class custom threshold τ_y

In our bias identification step, we customize the OCSVM algorithm, manipulating its decision function to accommodate a custom per-class decision threshold τ_y . These thresholds (different for each class) push the anomaly detectors to reject samples as out-of-class (*i.e.*, bias-conflicting) only when they are highly confident, and thus better discriminating between bias-aligned and bias-conflicting samples. In Table S.1, we report an ablation study on Corrupted CIFAR-10 (for three considered bias correlation values ρ), evaluating the impact of using our custom thresholds or exploiting the original formulation with the default threshold (which is 0).

Corrupted CIFAR-10	$\rho = 0.995$	$\rho = 0.980$	$\rho = 0.950$
Default threshold	23.21 ± 0.07	30.80 ± 0.17	37.88 ± 0.35
Per-class custom threshold (Ours)	27.26 ± 0.47	41.27 ± 0.26	50.48 ± 0.42

Table S.1: Average accuracies and standard deviations (over three runs) on Corrupted CIFAR-10, where we ablate the usage of custom decision thresholds in the OCSVM anomaly detectors employed in the proposed bias identification step.

non-biased CIFAR-10	Accuracy
ERM+CE	84.98 ± 0.35
MoDAD	82.87 ± 0.47

Table S.2: Impact of applying MoDAD on a model trained with the original version of CIFAR-10. Reported means and standard deviations are computed from three independent runs.

Although the default threshold can still provide reasonable debiasing performance, the proposed per-class custom thresholds lead to a significant improvement, ranging from about +4% to 13%, at the different bias levels. These results support our intuition on the necessity of obtaining a *purer* bias-conflicting prediction for improving debiasing performance.

S1.2 Sensitivity to different anomaly detection algorithms

In Figure S.1, we report the impact on Corrupted CIFAR-10 in terms of average accuracy of using different anomaly detection (AD) algorithms for bias correlation values $\rho = 0.980$ and $\rho = 0.995$ (in addition to the $\rho = 0.950$ case already provided in Section 4.4 of the main paper). The comparison involves the same algorithms indicated in the main paper, i.e. OCSVM, *Local Outlier Factor* [32], *Isolation Forest* [33], and *Robust Covariance Estimator* [34].

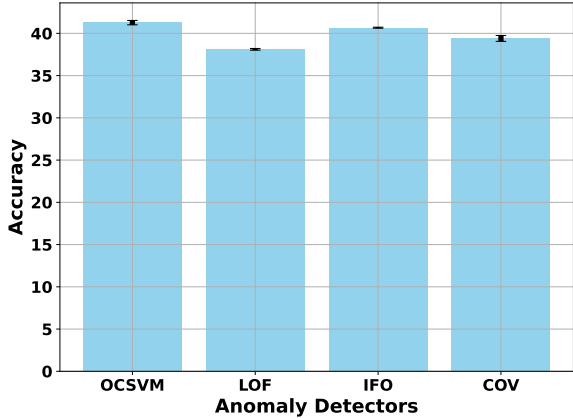


Figure S.1: $\rho = 0.980$.

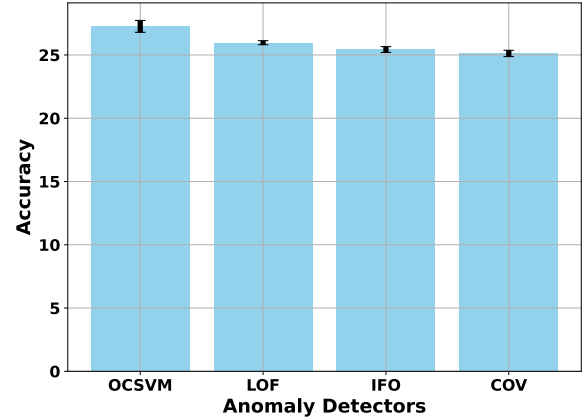


Figure S.1: $\rho = 0.995$.

Figure S.1: MoDAD average accuracy over three different runs with different anomaly detection algorithms on Corrupted CIFAR-10.

As already noticed for the $\rho = 0.950$ case, even with a higher bias correlation, there are no significant differences in performance among the several AD methods. We notice only a slight decrease in the performance for the explored detectors, which remains in the range of 2-3% with respect to the OCSVM. This empirically proves that even when the bias correlation level increases, different anomaly detectors behave similarly.

S1.3 MoDAD impact in case of non-biased datasets

Our method (MoDAD) is designed to be applied to a biased model, *i.e.*, on a model that fails to generalize even when properly trained and tuned, suggesting the presence of bias in data or dramatic distribution shifts. In such a case, MoDAD has a significant impact, succeeding in reducing the bias effect and debiasing the model. However, in general, we do not know whether a dataset is biased or not. Hence, we are interested in assessing the effect of MoDAD when applied to an unbiased model, *i.e.*, a model trained on an unbiased dataset. Thus, we run the two steps of MoDAD on the original non-biased version of CIFAR-10 and estimate average accuracy on the test set. As we can see in Table S.2,

Input Model	Average Accuracy
GCE Model	38.35 ± 0.35
Biased ERM	50.48 ± 0.62

Table S.3: MoDAD’s performance on Corrupted CIFAR10 ($\rho = 0.950$) with different input models for the debiasing step.

our debiasing method affects only slightly the performance on the test set with respect to the baseline ERM+CE trained model: we experience just a drop of $\sim 2\%$, which is significantly lower than the average benefit that we can get when using MoDAD on actually biased datasets.

S1.4 Input Model for the Debiasing Step

As reported in Section 3.3 of the main paper, our debiasing approach consists in fine-tuning a model trained with a vanilla ERM on the biased datasets. However, an alternative can be fine-tuning the intentionally biased model (trained with the GCE) utilized in the first step of our proposed approach. In Table S.3 we report a comparison between the two different input models for the debiasing step, on the Corrupted CIFAR-10 dataset (with $\rho = 0.950$). Fine-tuning the GCE model corresponds to a drop of $\sim 12\%$. This is expected, as the GCE model is intentionally and extremely biased by design, so it is more challenging to mitigate its bias dependency with respect to the biased Vanilla ERM model.

S2. Implementation Details

The code supporting this research and its experiments is implemented in Python [35], with the support of Pytorch and Torchvision [36, 37] for data pre-processing, neural network implementation, training, and evaluation. For the OCSVM algorithm (see Section 3 of the main paper), we rely on the open-source implementation available from Scikit-Learn [38]. Additionally, generic numerical operations and data visualization are performed exploiting Numpy [39] and Matplotlib [40] respectively.

S2.1 Data Pre-Processing

Input images are square-resized to a pixel resolution of 224x224 for BAR, Waterbirds, and BFFHQ. Corrupted CIFAR-10 images are instead kept at their original resolution of 32x32 pixels, following [12, 13, 4]. Regardless of the dataset, images are normalized to have RGB values between 0 and 1. Additionally, we replicate the same augmentations on the training images of Corrupted CIFAR-10, BAR, and BFFHQ that are found in [12, 13, 4], i.e.:

- **Corrupted CIFAR-10**
 1. RandomCropping((32, 32))
 2. Padding((4, 4))
 3. RandomHorizontalFlip(p=0.5)
- **BAR**
 1. RandomResizedCrop((224, 224))
 2. RandomHorizontalFlip(p=0.5)
 3. ImageNet Standardization
- **BFFHQ**
 1. Resize((224, 224))
 2. Padding((4, 4))
 3. ImageNet Standardization

During testing, we apply only square resizing and ImageNet standardization for BAR and BFFHQ. Concerning Waterbirds, we only perform square resizing of all input images with a target resolution of 224x224 pixels, followed by ImageNet standardization. We rely on Torchvision [37] for all the mentioned pre-processing operations.

S2.2 Training Details

In every experiment, we adopt AdamW as optimizer [41], with an initial learning rate of 10^{-5} for the debiasing step. For the bias-identification step involving GCE pre-training, we use an initial learning rate of 10^{-3} for Corrupted CIFAR-10 and 10^{-5} for the other datasets. The ERM models trained with Cross-Entropy loss (ERM+CE), are trained with a fixed learning rate of 10^{-3} and a mini-batch random sampler weighted on class populations. Regarding batch sizes, for the sake of fair comparisons, we follow what is found in the existing literature [12, 13, 1]: 256 for Corrupted CIFAR-10 and BAR, 128 for Waterbirds, and 64 for BFFHQ.

Network Embeddings. To extract the network embeddings employed in the proposed bias identification step (see Sec. 3.2 of the main paper), we consider the very last layer before the *softmax* layer that performs the final classification. This corresponds to the additional layer we attach to the ResNet backbone (see Training Details in Sec. 4.3 of the main paper), which is a *linear* layer with 128 neurons put after the ResNet’s last *pooling* layer, followed by a ReLU non-linearity. This is fixed regardless of the dataset and the backbone being a ResNet-18 (Corrupted CIFAR-10, BAR, BFFHQ) or a ResNet-50 (Waterbirds).

Training Iterations and Regularization. The bias-identification model trained with GCE loss is trained for 100 epochs in the case of Corrupted CIFAR-10, 30 epochs for BAR and BFFHQ, and 50 epochs for Waterbirds. The Debiasing step is performed for 100 epochs in the experiments for Corrupted CIFAR-10, while 50 epochs are employed for BAR, Waterbirds, and BFFHQ. We set a fixed number of epochs and do not employ any implicit regularization technique during training, as we cannot assume datasets-wise accordance regarding distribution shifts in the validation set.